Cationic nanogels based on diethylaminoethyl methacrylate

Steve R. Marek [a], Charles A. Conn [a,1], Nicholas A. Peppas [a,b,*]

[a] Department of Chemical Engineering, The University of Texas at Austin, Austin TX, USA
[b] Department of Biomedical Engineering, The University of Texas at Austin, Austin TX, USA

ARTICLE INFO

ABSTRACT

The effect of polymer composition and polymerization parameters such as comonomers, crosslinking ratio, and polymerization method, on the surface characteristics, surface chemistry, and swelling response of crosslinked 2-(diethylaminoethyl methacrylate) (DEAEM) and polyethylene glycol mono-ethyl ether monomethacrylate (PEGMMA) nanogels was studied. A novel inverse emulsion polymerization method was developed, which formed latex nanoparticles on the order of 100–400 nm. The properties of these nanogels were compared to microparticles synthesized via solution polymerization. The new polymerization method allowed the incorporation of PEG surface tethers of lengths 400 Da up to 2000 Da. Surface tethers successfully decreased the ζ-potential of these nanogels from 70 mV to 30 mV in acidic conditions and from −60 mV to 2 mV in basic media. Nanogels swelled from 100 nm in basic media to 800 nm in acidic media due to the protonation of the tertiary amine on DEAEM.

© 2010 Elsevier Ltd. All rights reserved.

1. Introduction

Nano-sized materials have attracted substantial interest over the last several years due to their unique characteristics and versatility. Nanoparticles, or more specifically nanogels (nanometer-scale hydrogels), have garnered some of this attention due to their wide range of uses, from applications such as paints and thickening agents [1,2], to drug delivery, diagnostics [3], and other biological applications. However, improved methods of production of such hydrogels are required. Here, a novel inverse emulsion polymerization is described for the synthesis of cationic nanogels that exhibit pH dependent swelling properties in aqueous environments.

The monomer 2-(diethylamino)ethyl methacrylate (DEAEM) is a well studied methacrylate monomer that easily undergoes free-radical polymerizations [4–6]. Several research groups have studied the macroscopic properties of hydrogels based on DEAEM, either as a homopolymer or copolymerized with such monomers as methyl methacrylate (MMA) [7], 2-hydroxyethyl methacrylate (HEMA) [8], and others [9,10]. These polymers have an increased hydrophilicity at pH values near and below the pK_a of the hydrogel due to the protonation of the tertiary amine. This process is reversible, and swellability decreases with increased pH.

Initial studies with poly(DEAEM) (PDEAEM) were performed by Shatkay and Michaeli [11], who identified the phase separation of PDEAEM at 7.48 and measured a pK_a of 7.68 via titration. Several factors can influence this pK_a value such as polymer chain length, comonomer composition (and thus hydrophobicity), and crosslinking ratio, with other researchers reporting values in the range of 7.0–7.4 [12,13]. These polymers also have a T_g below ambient temperature, with values ranging from 16 to 24 °C [7,14].

Previous reports have indicated that PDEAEM particle sizes can be reduced to the nanometer scale. However, most of these methods relied on the hydrophobicity of DEAEM to form emulsions [15–17] or precipitates. The incorporation of hydrophilic components on the interior of these nanogels was not considered, and in practice would be quite difficult with these methods due to the hydrophobicity of deprotonated DEAEM. These reactions also either took over 24 h or relied on UV initiation, both of which could inhibit the scale-up of such materials to more useful quantities.

The studies presented here examine the effects of a novel nanoparticle synthesis route of PDEAEM on several polymer properties, including surface charge and swelling response. A new inverse emulsion (water-in-oil) polymerization method is described. The effects of crosslinking ratio and polyethylene glycol (PEG) tether length on physical properties is also examined. The network morphology was also studied. These properties were compared to similar, macroscopically synthesized polymer particles to determine the difference between solution and emulsion polymerized particles. Finally, the potential for these systems to be used as drug delivery agents was evaluated.

* Corresponding author. Department of Chemical Engineering, The University of Texas at Austin, Austin TX, USA. Tel.: +1 512 471 6644; fax: +1 512 471 8227.
E-mail address: peppas@che.utexas.edu (N.A. Peppas).
[1] Present address: Department of Chemical Engineering, Rice University, Houston TX, USA.

2. Materials and methods

2.1. Poly(diethylaminoethyl methacrylate) polymer microparticle synthesis

Hydrogels of N,N-diethylaminoethyl methacrylate and poly (ethylene glycol)-n monomethyl ether monomethacrylate, henceforth P(DEAEM-g-EGn) were synthesized using a free-radical thermal polymerization in solution, where 'n' refers to the average molecular weight of the ethylene glycol repeat units (Fig. 1). To synthesize these systems, a solution of DEAEM (Sigma–Aldrich, St. Louis. MO), PEGnMMA (Polysciences, Warrington, PA) and the crosslinking agent tetraethylene glycol dimethacrylate (TEGDMA) or polyethylene glycol 400 dimethacrylate (PEG400DMA) (Acros Organics, Morris Plains, NJ) was made. The DEAEM was passed through a column of basic alumina (Fisher Scientific, Fair Lawn, NJ) prior to use to remove inhibitor. All other reagents were used as received. Phosphate buffered saline (PBS) (Fisher Scientific) was used as the solvent to prevent autoacceleration and was reconstituted from a $10\times$ concentrate with deionized water (Milli-Q Plus system, Millipore, Bedford, MA), in a ratio of about 1:1 by weight of the monomers. Hydrochloric acid (ca. 37 wt%, Fisher Scientific) was used to increase solubility. Ammonium persulfate (APS) (Fisher Scientific) and sodium metabisulfite (NaMBS) (Fisher Scientific) were used to initiate the polymerization in a ratio of 4:1 by mole, and the chemicals were pre-mixed before polymerization in distilled deionized water (ddH$_2$O) at a 1 wt% concentration of APS. The initiator solution was used in an amount of 0.5% by moles of monomers.

Several different systems were synthesized with varying compositions. The ratio of DEAEM to PEG grafts was either 10:1, 25:1, or no PEG grafts. Crosslinking ratios varied from 3 mol% up to 15 mol%. Once all compounds had been well mixed in a test tube, the solution was transported to a glove box where it was purged with nitrogen for 20 min to remove dissolved oxygen, a free-radical scavenger. The initiator solution was then added, mixed via aspiration, and then pipette between two glass slides, separated by a 760 μm Teflon spacer. The glass slide assembly was then placed in an acrylic air-tight polymerization box, sealed, and transported to an incubator at 37 °C for 24 h. This procedure resulted in polymer films which were crushed into microparticles via a wet-sieving technique. The samples were then washed in a jar of PBS for one week to remove unreacted monomers and small molecular weight polymers. The polymers were then either stored in buffer or freeze-dried (particles) and stored in a dessicator until use. These hydrogels were used as a comparison for the nanoparticles.

2.2. Poly(diethylaminoethyl methacrylate) nanoparticle synthesis

Nanoparticle hydrogels of P(DEAEM-g-EGn) were synthesized using a free-radical thermal inverse emulsion polymerization. The accelerant N,N,N′,N′-tetraethylmethylenediamine (TEMED, Fisher Scientific) allowed the reaction to proceed at room temperature, and a 2:1 molar ratio of Brij® 30 to Triton®; X-100 was used. In a routine polymerization, 85 mL of cyclohexane (Fisher Scientific) was added to a round bottom flask containing 4.7 g Brij 30 and 8.7 g Triton X-100. The aqueous monomer solution, prepared as stated above, was then added to the flask. The mixture was homogenized (Ultra-Turrax T25, IKA, Wilmington, NC) at 24,000 rpm for 5 min. The emulsion was then purged with N$_2$ for 20 m to remove dissolved oxygen, after which 0.35 mL of TEMED were injected. Particles of about 220 nm (collapsed) were formed. The cyclohexane was removed under reduced pressure and the particles were precipitated with ethyl ether (Fisher Scientific) three times, using centrifugation to pellet the nanogels. The particles were then washed for one week in a dialysis membrane (14 kDa cutoff, SpectraPor, Spectrum Laboratories, Inc., Rancho Dominguez, CA) and the dialysate was changed twice a day. After the washing steps were completed, the particles were lyophilized on a Freezone freeze dryer (Model 77500, Labconco Corp., Kansas City, MO) and stored in a desiccator until use.

2.3. FT-IR spectroscopic analysis

Fourier transform infrared (FT-IR) spectra were obtained on a ThermoNicolet Nexus 470 spectrometer (Thermo Electron Corp., Waltham, MA) with a deuterated triglycine sulfate (DTGS) detector and potassium bromide (KBr) beam splitter. Typically, 128 scans were performed in the wavenumber range of 4000–400/cm, both forward and backward at 10 kHz, with a manual gain of one. Pellets of ca. 10 mg polymer and 200 mg KBr (spectroscopy grade, Acros Organics) were pressed at 15,000 psi using a Carver laboratory press. Either crushed microparticles or nanoparticles were used for the spectra.

2.4. NMR spectroscopy

Nuclear magnetic resonance (NMR) spectra were obtained on a Varian Unity+ 300 MHz spectrometer. Deuterated water (D$_2$O, Cambridge Isotope Laboratories, Inc., Andover, Ma.) was used to suspend nanoparticles for tether analysis. Water suppression was used via the PRESAT macro with a saturation power of −2 and a saturation time of 5 on any samples with significant water signals. Small molecule analysis was obtained by using a suitable deuterated solvent, such as chloroform (CDCl$_3$), dimethylsulfoxide (d_6-DMSO), or d_6-acetone, all obtained from Cambridge Isotope Laboratories. Unless otherwise stated, for all ^{1}H NMR spectra, the sample was spinning at 20 Hz, the number of transients was 8, and line broadening was 0.1.

2.5. Differential scanning calorimetry (DSC)

A PerkinElmer DSC 7 differential scanning calorimeter (PerkinElmer, Waltham, MA) using a heat/cool/heat method was used to characterize the polymers, both nanoparticles and crushed microparticles. A rapid heating cycle was used to erase any thermal history from the samples, after which the samples were cooled back down to the starting temperature. The final heating cycle had a ramp rate of 10 °C/min, which was slow enough to detect a T_g in
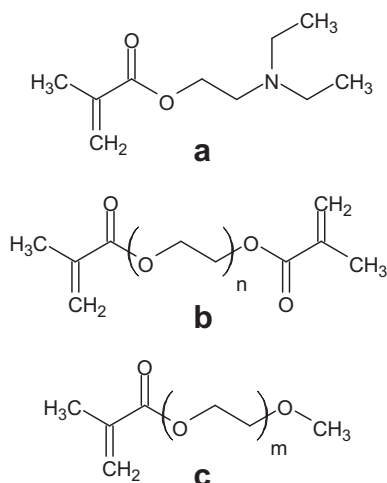

Fig. 1. Monomers used in the synthesis of P(DEAEM-g-EGn). (a) DEAEM, (b) PEGDMA-n, n = 4 for TEGDMA, n = 8 for PEGDMA400, (c) PEGMMA-n, n = 8 for PEGMMA400, n = 22 for PEGMMA1000, n = 45 for PEGMMA2000.

some samples. Since room temperature was above the T_g of most samples, a nitrogen cooling unit was used with an initial temperature of −55 °C.

2.6. Dynamic light scattering (DLS) and ζ-potential

Nanoparticle hydrodynamic diameters were characterized using a ZetaPlus Zeta Potential Analyzer with a Multi Angle Particle Sizing Option installed (Brookhaven Instruments Corporation, Holtsville, NY) operating with a 25 mW laser at a wavelength of 635 nm. Detection of scattered light was at 90° to the incident beam. Each sample was subjected to 10 two-minute measurements. Typically, solutions of up to 2 mg/mL were used for the characterizations, at a temperature of 25 °C. Freeze-dried particles were suspended in either PBS or 2 mM KCl. The pH of the nanoparticle solution was altered with either 0.1 N HCl or 0.1 N NaOH (Fisher Scientific), and was measured with an ISFET probe using an IQ Scientific Instruments pH meter.

ζ-Potential measurements were conducted on nanoparticles using electrophoretic light scattering, also using the Brookhaven ZetaPlus. Freeze-dried particles were suspended in a 10 mM KCl solution and diluted to 2 mM KCl with ddH$_2$O. Scattered light was detected at 15° (175° to the incident beam) at a temperature of 25 °C. Each sample was subjected to 10 measurements, with a 5 s delay between each measurement. The pH of the medium was controlled with dilute HCl or NaOH, and nanoparticle measurements were initially taken at basic conditions and the pH was lowered for each subsequent measurement.

2.7. Scanning electron microscopy (SEM)

A LEO Model 1530 SEM was used to determine the morphology of the synthesized particles. To prevent charging of the samples, samples were sputter coated with a 10 nm gold layer using a Pelco Model 3 sputter coater (Pelco International, Redding, CA). Stages were stored in a dessicator until loading into the SEM due to the hygroscopic nature of protonated DEAEM.

2.8. Microparticle swelling characterization

As stated above, nanoparticles were sized via DLS as a function of pH. The swelling response of microparticles was obtained gravimetrically and used as a comparison to the swelling response of the nanoparticles. The polymer samples were titrated to the desired pH with either 0.1 N HCl or 0.1 N NaOH, and the pH was measured with an ISFET probe as with the nanoparticles. Swelling media was PBS with an ionic strength of 154 mM and initial pH of 7.4. Microparticles were centrifuged at a relative centrifugal force of 3200 g (Centra CL3R, Thermo IEC) and the supernatant was removed to obtain the mass of the particles.

3. Results and discussion

3.1. Poly(diethylaminoethyl methacrylate) polymer microparticle synthesis

Films, which were then crushed into microparticles, were successfully synthesized. Wet sieving yielded irregularly-shaped particles with sizes of sub-150 μm or sub-45 μm in the relaxed state, depending on which sized sieve was used. It is necessary to note that all systems in this work are referred to by their feed (pre-polymerization) compositions rather than polymer compositions due to the difficulty in quantitatively analyzing crosslinked copolymer compositions. These microparticles were then used in subsequent studies as a comparison to the nanoparticles.

3.2. Poly(diethylaminoethyl methacrylate) nanoparticle synthesis

Sub-micron sized particles, or nanoparticles, were successfully synthesized via this novel inverse emulsion polymerization procedure. The necessity for an inverse emulsion stems from the desire for these particles to contain hydrophilic components, such as PEG surface tethers and possibly either proteins or enzymes on the nanogel interior. Previous synthetic approaches inhibited the incorporation of such hydrophilic components due to the hydrophobicity of deprotonated DEAEM. Thus, monomeric DEAEM and hydrophilic comonomers (i.e., functionalized enzymes), did not properly copolymerize. Using this novel polymerization method will allow the copolymerization of DEAEM with several hydrophilic monomers, including functionalized enzymes such as glucose oxidase for the detection of glucose in solution.

It was determined that a 2:1 molar ratio of nonionic surfactants Brij 30 (Sigma) and Triton X-100 (Sigma) was able to form a stable inverse emulsion and provide fairly monodisperse nanogels. This result is somewhat contrary to theory, since the hydrophile–lipophile balance (HLB) of each surfactant is 9 and 13.5, respectively (as provided by the manufacturer). The HLB is a quantification of the ratio of hydrophilic to lipophilic functional groups in the surfactant, where surfactants with values < 10 typically form inverse emulsions, and surfactants with values ≥ 10 form stable emulsions (oil-in-water). Ionic surfactants were investigated, though several problems were encountered. Select cationic surfactants (e.g. MyTAB) would not form inverse emulsions, and anionic surfactants (e.g. AOT) complexed with the partially protonated DEAEM monomers, which prevented proper polymerization.

3.3. FT-IR spectroscopy

FT-IR showed the functional groups present in each sample which indicated the successful removal of unreacted double bonds. The C=C stretching absorbance near 1650 cm^{-1} and the out-of-plane C–H bending of these same double bonds near 950 cm^{-1} were nearly non-existant. Also, the larger presence of etheric bonds in the samples containing PEG tethers, near a frequency of 1100 cm^{-1} (C–O stretching), indicates a higher content of PEG than those simply containing PEG crosslinker. Thus, it is reasonable to assume that the PEG tethers were successfully incorporated into the hydrogel backbone.

3.4. NMR spectroscopy

Water suppression was necessary for all samples analyzed in D$_2$O; otherwise, the signal-to-noise ratios for the hydrogel peaks were too low for analysis. ^{1}H NMR was used to confirm the presence of PEG tethers on nanogels in D$_2$O by identifying the PEG oxyethylene peak at about 3.6 ppm. As the PEG tether length or PEG ratio was decreased, the area of the oxyethylene peak also decreased and was practically non-existent in the spectrum of nanogels synthesized without PEG tethers. Lightly crosslinked nanogels were used in these analyses, which also allowed the observance of PDEAEM peaks as well (3.2 ppm, 3.5 ppm). However, directly comparing the PEG oxyethylene peak to the methylamine peak on DEAEM did not provide an accurate assessment of the ratio of DEAEM to PEG surface grafts due to limitations of NMR on crosslinked nanoparticles.

3.5. Differential scanning calorimetry (DSC)

Heat flow curves as a function of temperature were generated for several different polymeric systems (Fig. 2). P(DEAEM-g-EG2000) nanogels exhibited a peak T_m at 47 °C, which is
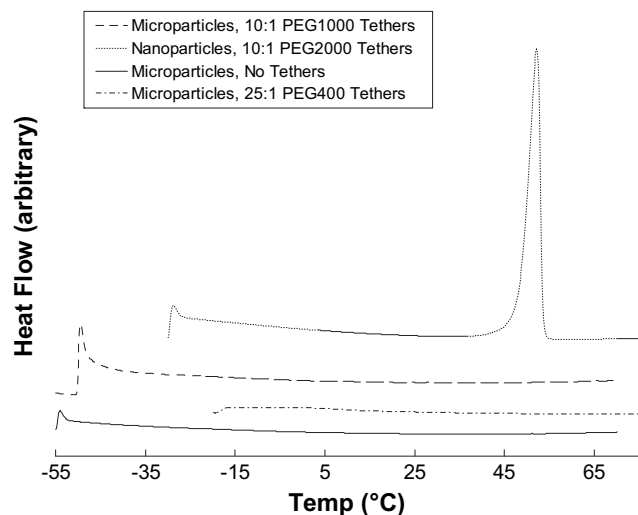
Fig. 2. Differential scanning calorimetry heat flow curves. Heat flow curves indicating a lack of T_g for all particles. The top curve indicates the existence of crystalline PEG due to the surface-grafted PEG tethers of the nanoparticles.

consistent with the melting temperature of pure PEG at a molecular weight of 2000 Da. These results are further evidence of the inclusion of PEG tethers on the nanogel surface, where tethers from several particles crystallized during the freeze-drying process. Using the melting peak for PEG allowed the calculation of the initial PEG crystallization amount to be about 30% for PEG2000 tethers, which could be recrystallized to 50% after a melt–freeze cycle; the enthalpy of melting values were obtained from Sanchez-Soto et al. [18]. These values assume near 100% conve rsion of PEG monomer, which may not be accurate.

It is interesting to note that crushed microparticles with the same composition did not have an observable T_m. This result can be explained by the methods of polymerization and how they alter the polymer structure. The crushed microparticles were synthesized as a film, where the PEG and DEAEM copolymerized without any partitioning. The nanogels, however, experienced PEG partitioning into the surfactant layer. Thus, PEG was more likely to polymerize near the surface of the polymer particles than on the inside. This phenomenon resulted in more PEG protruding from the surface of the nanogels than from the microparticles. These PEG tethers were then able to crystallize with each other during the freeze-drying process. Crystallization did not occur with nanoparticles containing shorter PEG tethers.

The T_g of crosslinked hydrogels was unable to be determined, due to the highly restricted polymer chain motion from the crosslinking. Neither nanogels nor microparticles exhibited a detectable T_g, However, the T_g of uncrosslinked PDEAEM was determined to be −20 °C, which agrees with previous reports.

3.6. DLS and ζ-potential

DLS provided the solvated hydrodynamic diameter of nanoparticles as a function of pH. Similar to the crushed particles, the transition pH from collapsed to swollen occurred over a narrow range of about 7.4. Due to the limitations of DLS, the swelling properties of some nanogels were not fully investigated. The ability of DLS to measure particle size is dependent on the scattering of laser light off the polymer surface. However, as the nanogels swell with water, the polymer volume fraction can be as low as 1%. Thus, the polymer gel is almost completely solvent (polymer volume fraction approaches zero), and it is difficult for the laser to scatter enough light to collect reliable data. An increase in polymer

concentration can help increase the signal-to-noise ratio, but this step also increases the viscosity of the solution drastically, which has also been shown to produce errant values for particle dimensions [19]. The nanogel suspension was first measured in a viscometer to reduce the possibility of this error.

Several important observations were made via DLS. As shown in Fig. 3 the swelling response of DEAEM based nanogels was not significantly affected by the presence of PEG tethers. When the crosslinking ratio was held constant, both systems had a transition from collapsed to swollen state at a pH of about 7.2, which agrees with previous reports on similar systems. The particle size in the collapsed state for the non-PEGylated systems was, however, larger than those with surface PEG tethers. This phenomenon was most likely due to slight aggregation, since the deprotonated DEAEM was fairly hydrophobic without PEG tethers. Nanogels viewed in their dried state tended to have very similar "collapsed" diameters as shown by SEM below. Finally, as mentioned above, as the polymers swelled at low pH, the standard deviation between measurements increased, mainly due to the difficulty in sizing via DLS at such conditions.

The ζ-potential of the nanoparticles was shown to be affected by PEG tether length (Fig. 4). The longer PEG chains were able to more effectively shield the surface charge of the polymers, thus reducing the measured ζ-potential at all pH values. It has been shown previously that solvated ions may preferentially adsorb to a solvated surface, imparting a strong positive or negative charge to the surface [20,21]. Thus, in basic media, the obvious ion imparting a negative charge was hydroxide. These negative charges at elevated pH values are most likely not due to hydrolysis of the ester groups on each DEAEM repeat unit into polymethacrylic acid since the ζ-potential measurements were performed from basic to acidic pH values, and this negative charging was reversible.

The PEG tethers were highly effective at preventing free hydroxide ions from adsorbing to the polymer surface at higher pH ranges. The PEG tethers acted like a molecular brush, preventing the adsorption of dissolved ions onto the polymer surface. Thus, there was a reduction in the overall surface charge, especially at higher pH values, which can be exploited for biological applications such as drug delivery.

PEG also successfully shielded the positive charges on the protonated amines along the polymer background. However, this shielding effect was less than that of the hydroxide ions at basic pH values. This trend is most likely explained by the nature of PEG and ζ-potentials. PEG is highly effective at preventing ions, proteins, and other molecules from adsorbing to a surface. However, this effect is not fully able to shield the positively charged polymer due to the
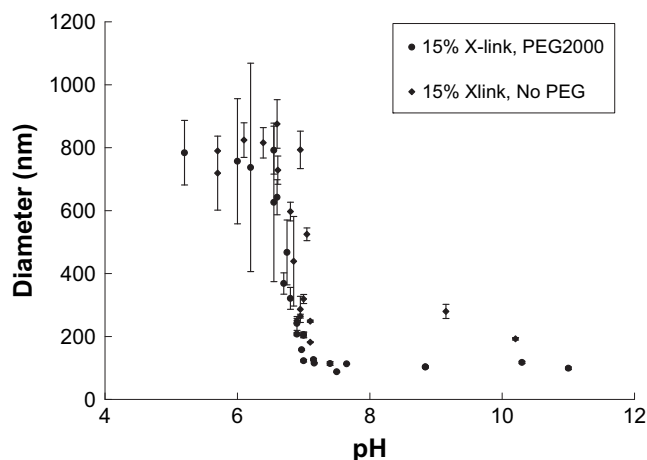

Fig. 3. Volume swelling ratios of nanoparticles as measured by DLS.
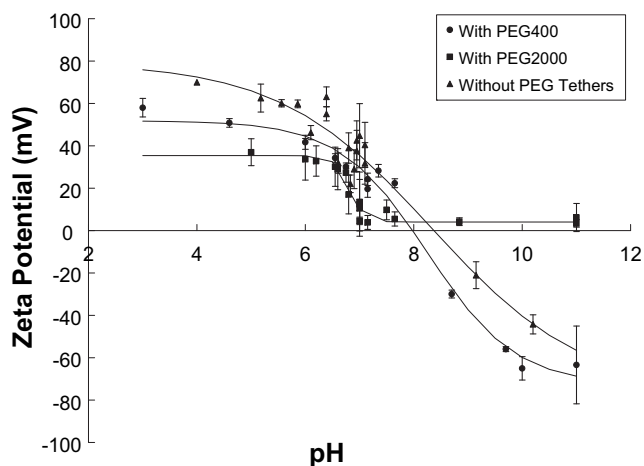
Fig. 4. Zeta potential as a function of pH for several polymer nanoparticles. PEG tether length and content decreased the overall surface charge.

electric double layer present around such a material. Even longer PEG chains should increase the gap between the polymer and this double layer, thus reducing the ζ-potential. However, there is a practical limit to the PEG tether length due to the polymer synthesis method. Finally, the total number of PEG tethers on the surface of a given particle does not change with swelling, yet the surface area increases by radius squared. Thus, PEG tethers comprise more surface area of the nanogel when in the collapsed state versus the swollen state.

Previous work has shown that the incorporation of PEG tethers can have substantial benefits, such as increased suspension stability and decreased surface adsorption [22]. Moghimi *et al.*, showed that PEG grafts of at least 2000 Da were necessary to prevent protein adsorption, while weights over 5000 Da further decreasing overall effectiveness [23]. These observations are consistent with the data above, indicating that PEG tethers of molecular weight 2080 Da were ideal for preliminary studies. Future studies could examine the effect of a tether longer than 2000 Da.

3.7. Scanning electron microscopy (SEM)

Several important observations can be made from the SEM micrographs shown in Fig. 5. The nanoparticle synthesis provided fairly monodisperse samples, with only slight variations in size from particle to particle. These micrographs confirm particle size determinations via DLS to be on the order of 200 nm for collapsed particles. While these particles were freeze-dried prior to imaging and do not directly provide collapsed particle sizes in solution, these data do agree well with data obtained from the light scattering method.

There is a noticeable difference between nanoparticles synthesized with PEG tethers versus those without. The surface characteristics of the nanoparticles with PEG tethers appear to be softer and more diffuse (Fig. 5b and c), whereas particles without tethers appear to have more rigid boundaries. This phenomenon could be explained by the hair-like protrusion of the PEG tethers from the surface of the particles, providing a more textured surface for the sputter coated gold layer to adhere to, which in turn could have caused decreased localized resolution. It was reported that PEG tethers of 2000 Da could extend past the particle surface by as much as 7 nm based on the Flory radius of these tethers [24]. The low glass transition temperature of the PEG tethers also may play a role in this observation.

The low glass transition temperatures of the PDEAEM polymers offered an extra challenge during imaging. Deprotonated PDEAEM has a T_g below room temperature, whereas protonated PDEAEM has a somewhat higher T_g. Thus, deprotonated PDEAEM is rubbery and
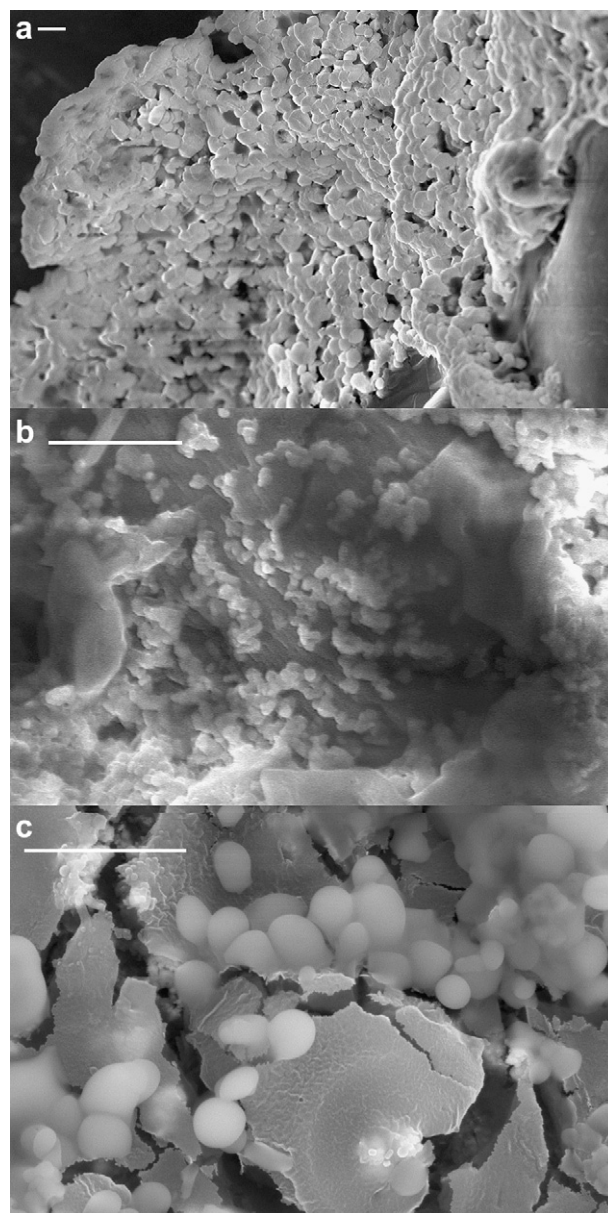

Fig. 5. SEM micrographs of different nanogels: a) PDEAEM without PEG tethers; b) P(DEAEM-g-EG1000) with a 25:1 DEAEM:PEG ratio; c) P(DEAEM-g-EG2000) with a 10:1 ratio of DEAEM:PEG. All scale bars are 2 μm.

likely to deform during sample preparation and coalesce into a film, making imaging of distinct particles difficult if not impossible. Protonated PDEAEM, on the other hand, has a higher T_g making it glassy at room temperature. This characteristic allows better imaging at the expense of the increased hygroscopic nature of the polymer. These observations agree with previously reported results, which also indicate the difficulty in preventing latex films of PDEAEM during the sample preparation process [17]. Cornejo-Bravo and Siegel quantified the hygroscopic nature of dry, deprotonated PDEAEM by measuring the amount of water vapor absorbed from the air. Polymer weight doubled, and the water acted as a plasticizing agent.

3.8. Microparticle swelling characterization

Swelling analyses of the microparticle systems showed a sigmoidal response to pH as expected (Fig. 6), with the transition
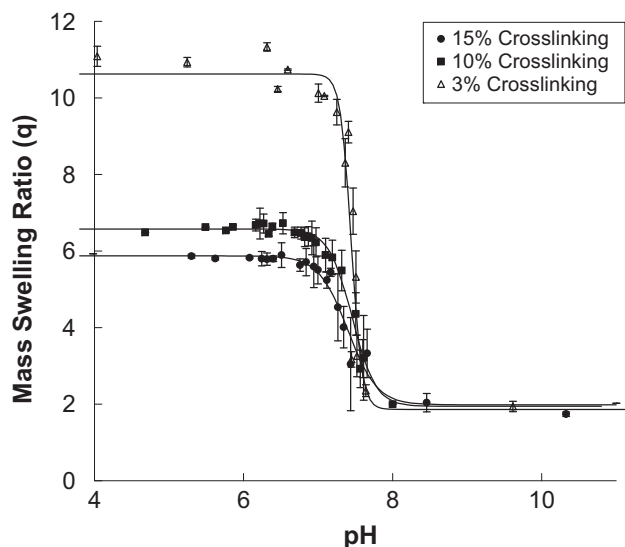
Fig. 6. Weight swelling of crushed microparticles (150 μm) as a function of pH. An increase in the crosslinking of the polymers reduced the overall swelling, reducing the amount of water uptake. The lines are sigmoidal regressions of the data.

occurring rapidly near the pK_a of the polymer. The pK_a of DEAEM polymers is a function of molecular weight, comonomer composition, and to some degree, temperature, with a range between pH 7.0–8.0. At 25 °C the transition from fully collapsed to fully swollen occurs over a narrow pH range of less than 1 unit and occurred at about pH 7.2 (Fig. 6). This pK_a range is important in several applications, most notably in biological systems which are typically buffered at a near neutral pH.

Swelling results for microparticles are reported here as a weight swelling ratio (q),

$$q = W_s/W_d,$$

where W_s is the swollen weight of the particles and W_d is the dry weight of the particles. Even when fully collapsed, particles retained about equal masses of polymer and solvent, resulting in a collapsed q of 2. As crosslinker content increased, the overall mass swelling decreased due to restrictions in interchain movement. Polymers with a 15% crosslinking ratio swelled from a collapsed weight swelling ratio of 2 (q, weight swollen divided by weight dry) to a ratio of 6, samples that had 10% crosslinking ratio swelled to a ratio of 6.6, while samples that were only crosslinked at 3% swelled to a ratio of 11. Solid lines represent a sigmoidal (hyperbolic tangent) fit to the data, and not just a guide to the eye. These data agree with previous reports of similar systems [16,25,26].

These swelling values were then used to estimate the mesh size of each sample. Since the mesh size of a hydrogel is essentially the molecular pore size, it can be used to help determine the ability of a given solute to diffuse through the polymer. There are several methods of estimating the mesh size of a hydrogel; however, the Flory–Rehner model was selected due to the difficulty of measuring such parameters as the relaxed volume (i.e., for the Peppas–Merrill or Brannon–Peppas equation). Thus, these values are rough estimates of the actual values and should not be taken as the actual values themselves.

To determine the polymer parameters, hydrogels were swollen to equilibrium and then mass swelling was determined. The ratio of swollen mass to dry mass, q, was calculated for each data point, and the polymer volume fraction in the swollen state, $v_{2,s}$, was calculated with Equation (1):

$$v_{2,s} = \frac{m\overline{v}}{m\overline{v} + mq/\rho_w} \tag{1}$$

where m is the mass of dry particles, $\overline{v}$ is the specific volume of the polymer (0.93 g/cm^3), and ρ_w is the density of water.

For the reasons mentioned above, estimation of the average molecular weight between crosslinks was performed by using the Flory–Rehner model:

$$\frac{1}{\overline{M}_c} = \frac{2}{\overline{M}_n} - \frac{\left[\ln(1 - v_{2,s}) + v_{2,s} + \chi_1 v_{2,s}^2\right]}{\left(\frac{V_1}{\overline{v}}\right)\left[v_{2,s}^{1/3} - \frac{v_{2,s}}{2}\right]} \tag{2}$$

The parameters are as follows: V_1 is the molar volume of the swelling agent (18 cm^3/mol for water), I is the ionic strength (1.7 for PBS, 0.002 for 2 mM KCl), χ_1 is the Flory polymer–solvent interaction parameter (0.2, as estimated by Hariharan [8]), and $\overline{M}_n$ is the number average molecular weight of the polymer chains before crosslinking (estimated to be 15 kDa by GPC, though the actual value has negligible influence on estimates beyond a certain value). Once $\overline{M}_c$ was know, the mesh size (ξ) was calculated from Equation (3),

$$\xi = v_{2,s}^{-1/3}\left(\frac{C_n\overline{M}_c}{M_r}\right)^{1/2} l \tag{3}$$

where C_n is the Flory characteristic ratio (14.6 for vinyl polymers), M_r is the average molecular weight of the repeat units, and l is the length of the bond along the polymer backbone (1.54 Å for vinyl polymers).

The results of this analysis are as follows and shown in Fig. 7. Microparticles with a crosslinking ratio of 15% had, as expected, the smallest swollen mesh size at a value of 34 Å. As the crosslinking ration decreased, the hydrogels formed larger molecular pores with values of 40 Å for a 10% crosslinked sample and 68 Å for the 3% crosslinked sample. All samples had a collapsed mesh size on the order of 1 Å. Therefore, it should be feasible to entrap medium molecular weight compounds in the collapsed state, and allow controlled release of these compounds in the swollen state. Small peptides, such as insulin with a monomeric radius of only 1.3 nm [27], should have no trouble being imbibed into the network and then trapped upon collapse. These estimates could also be applied towards the nanoparticle systems, yielding similar results.

4. Conclusions

Hydrogels, in the forms of microparticles and nanoparticles, were successfully synthesized using a redox initiated free-radical polymerization. A novel inverse emulsion polymerization method was described, which allowed nanogels on the order of 200 nm to be synthesized. These systems were characterized by several different techniques. FT-IR confirmed functional group content. ^{1}H NMR indicated successful copolymerization of PEG which resulted in soluble tethers protruding from the surface of the nanogels. DSC indicated the lack of a discernable T_g in these highly crosslinked systems but also confirmed PEG tether content. DLS was used for nanoparticle sizing, though limitations of the equipment were observed which prevented the complete analysis of certain systems. SEM micrographs confirmed that particle sizing measurements provided by DLS were accurate. Surface features were also elucidated, indicating that PEG provides different surface properties in the dried state.

As mentioned in the ζ-potential results above, the PEG tether length directly affected the observed ζ-potential of the nanogels. Longer chain lengths provided better shielding for the positive
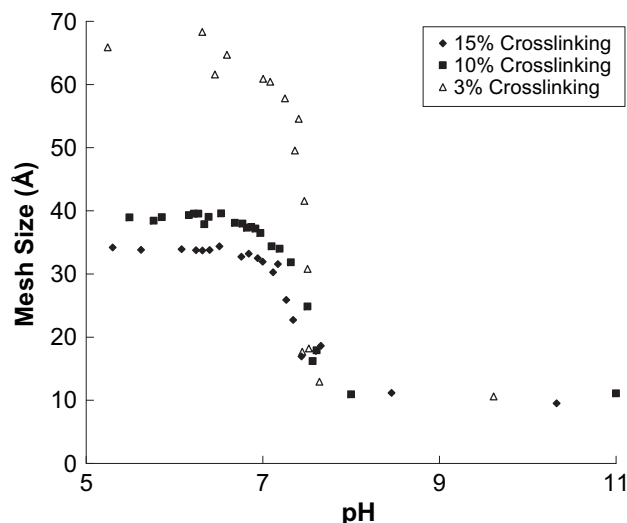
Fig. 7. Mesh size estimations as a function of pH for crushed microparticles (150 μm). Initially, all three sets of microparticles remained collapsed at a mesh size of 1 nm, small enough to entrap small peptides and other such molecules.

charges on the polymer backbone. However, a PEG molecular weight of 2000 Da was the largest PEG tested. The possibility of a longer PEG chain providing better shielding for the protonated amines may be worth investigating in future studies.

These studies have demonstrated that all PDEAEM-based systems synthesized exhibit a sigmoidal response to changes in pH. With this increase in polymer volume, the mesh size increased, and an increase in the diffusion rate of solutes should be present. Thus, these systems are ideal candidates for applications such as controlled drug delivery of medium-sized molecules such as small peptides. The loading and release properties of drugs with these systems need to be characterized to determine their feasibility in a drug delivery application. Finally, since a novel nanogel synthesis was created using inverse emulsion polymerization, the option for including hydrophilic comonomers during polymerization is possible. Thus, molecules such as functionalized enzymes (i.e., glucose oxidase) can successfully be incorporated into these systems, allowing environmentally responsive systems capable of swelling and deswelling in the presence of an analyte.

References

[1] Hellgren A-C, Weissenborn P, Holmberg K. Progress in Organic Coatings 1999;35(1–4):79–87.
[2] Rodriguez BE, Wolfe MS, Fryd M. Macromolecules 2002;27(22):6642–7.
[3] Bromberg L, Salvati L. Bioconjugate Chemistry 1999;10(4):678–86.
[4] Kost J, Langer R. Equilibrium swollen hydrogels in controlled release applications. In: Peppas NA, editor. Hydrogels in medicine and pharmacy. Boca Raton, Fla: CRC Press; 1986. p. 95–107.
[5] Siegel RA, Firestone BA. Macromolecules 1988;21(11):3254–9.
[6] Siegel RA, Firestone BA, Johannes I, and Cornejo J. Abstracts of Papers of the American Chemical Society 1990;199:119–POLY.
[7] Cornejo-Bravo JM, Siegel RA. Biomaterials 1996;17(12):1187–93.
[8] Hariharan D, Peppas NA. Polymer 1996;37(1):149–61.
[9] Podual K, Doyle FJ, Peppas NA. Biomaterials 2000;21(14):1439–50.
[10] Schwarte LM, Peppas NA. Polymer 1998;39(24):6057–66.
[11] Shatkay A, Michaeli I. The Journal of Physical Chemistry 1966;70(12):3777–82.
[12] Bune YV, Sheinker AP, Kozlova NV, Abkin AD. Polymer Science U S S R 1981;23(8):2019–24.
[13] Butun V, Armes SP, Billingham NC. Polymer 2001;42(14):5993–6008.
[14] Tobolsky AV, Shen MC. The Journal of Physical Chemistry 2002;67(9):1886–91.
[15] Hayashi H, Iijima M, Kataoka K, Nagasaki Y. Macromolecules 2004;37(14):5389–96.
[16] Fisher OZ, Peppas NA. Macromolecules 2009;42(9):3391–8.
[17] Amalvy JI, Wanless EJ, Li Y, Michailidou V, Armes SP, Duccini Y. Langmuir 2004;20(21):8992–9.
[18] Sanchez-Soto PJ, Gines JM, Arias MJ, Novak C, Ruiz-Conde A. Journal of Thermal Analysis and Calorimetry 2002;67(1):189–97.
[19] Malvern. The importance of sample viscosity in dynamic light scattering measurements. Application note. Recognising the quality of data from photon correlation spectroscopy measurements. Technical note.: Malvern Instruments; 2005.
[20] Schweiss R, Welzel PB, Werner C, Knoll W. Langmuir 2001;17(14):4304–11.
[21] Jesionowski T. Colloids and Surfaces A-Physicochemical and Engineering Aspects 2003;222(1–3):87–94.
[22] Owens DE, Peppas NA. International Journal of Pharmaceutics 2006;307(1):93–102.
[23] Moghimi SM, Hunter AC, Murray JC. Pharmacological Reviews 2001;53(2):283–318.
[24] Wong JY, Kuhl TL, Israelachvili JN, Mullah N, Zalipsky S. Science 1997;275(5301):820–2.
[25] Podual K, Doyle FJ, Peppas NA. Polymer 2000;41(11):3975–83.
[26] Podual K, Peppas NA. Polymer International 2005;54(3):581–93.
[27] Oliva A, Fariña J, Llabrés M. Journal of Chromatography B: Biomedical Sciences and Applications 2000;749(1):25–34.